FROM BIOMASS TO WEARABLE DEVICES: LASER-INDUCED GRAPHENE DERIVED FROM LIGNIN FOR ULTRASENSITIVE SENSING

A Thesis presented to the Faculty of the Graduate School

University of Missouri – Columbia

In Partial Fulfillment of the Requirements for the Degree

Master of Science

By

Shuhong Yang

Dr. Caixa Wan, Thesis Supervisor

July 2021

The undersigned, appointed by the dean of the Graduate School, have examined the thesis entitled:

From Biomass to Wearable Devices: Laser-Induced Graphene Derived from Lignin for Ultrasensitive Sensing

Presented by Shuhong Yang,

a candidate for the degree of Master of Science in Biological

Engineering, and hereby certify that, in their opinion, it is worthy of acceptance.

_____

Professor Caixia Wan, Biological Engineering

_____

Professor Yi Zhang, Biological Engineering

_____

Professor Jian Lin, Mechanical Engineering

ACKNOWLEDGMENTS

I would like to thank my advisor and thesis supervisor, Dr. Caixia Wan, for guiding me with research direction, encouraging me throughout the research process, and offering me with great support and help.

I would like to thank Dr. Yi Zhang for serving as my co-advisor and Dr. Jian Lin for severing on my committee member. Thanks for their time and advice on my thesis.

Many thanks go to my lab mates: Hanwen Zhang, Wenjun Fan, Yisheng Sun, Qianwei Li, Krishanthi Mapa Mudiyanselage, Nan Zhao, and Jiayue Chen for their help. A special thanks goes to Dr. Zheng Yan and Yun Lin for all the help and suggestions on my research project.

I would also like to thank my parents for their love and support during my graduate study.

Table of Contents

ABSTRACT

Laser-indued graphene (LIG) is 3D porous structure with many promising properties. Lignin-based precursor has shown its unique properties in generating high quality LIG among various organic carbon-based substrates. In this study, we explored LIG derived from lignin for an ultrasensitive strain sensor for the first time. The main procedures included the precursor preparation, laser writing process, sensor fabrication, sensitivity test to strains and vibrations, and performance test on human body. The results demonstrated an excellent performance of our strain sensors with high accuracy and ultrasenstivity, suggesting the promising future of lignin valorization into LIG and futher wearable devices.

Chapter I Introduction

1.1 Background

Laser-induced graphene (LIG) can be induced from various precursors via direct laser writing. It has many good chemicals, physical, and electronic properties, like chemical resistance, thermal stability, and conductivity. More importantly, it has been used for many applications, like physical and chemical sensors(Cheng et al., 2016; Jeong et al., 2019), micro-supercapacitors(Mahmood et al., 2020), microfluidic devices(Griesche et al., 2021), electrocatalysts(Ye et al., 2019). The easy and low cost LIG producing process allows itself for scalable manufacturing in widespread industrial applications. Mainly, there are four kinds of applications based LIG technology, such as sensors, supercapacitors, microfluidic devices, electrocatalyst.

For LIG-based sensor applications, the working mechanism of a flexible wearable electronic sensors is that the external stimulus would be reflected by the relative changes of some electrical parameters. For example, in one previous study, one team had created a wearable, artificial throat based on LIG induced from PI to detect and generate sounds. The mechanism of detecting sound was based on the piezoelectric effect and inverse piezoelectric effect(Tao et al., 2017). Notably, the working principle for sound generation was established on database and machine learning, because when different physical pressure was applied, the sensor would generate characteristic waveforms. In another previous study, one group had developed a sensor that can monitor heart rate, body surface temperature, blood oxygen level, exercise volume, and other physiological parameters as well as monitor important physiological indicators related to inflammation and even insulin (Chun et al., 2019).

When it comes to chemical sensors, generally, there are two main principles of LIG-based chemical sensor applications: binding effect and redox reaction. The binding effect refers to the specific binding of chemical substances to the LIG surface that can transform the external stimulus into electrical signals. The non-specific binding detection approach is based on a redox reaction to cause a transformation of charge transfer resistance between electrolyte and electrode surface. Zhang and his team produced immobilized aptamers onto plasma treated LIG as the electrodes probe. When BPA was combined with the electrode surface, the capacitance between the electrodes and its surface would be decreased (Z. C. Zhang et al., 2018). In another study, LIG produced from PI had been designed as a 3-electrode system used to monitor the concentration change of chloramphenicol (CAP). The CAP concentration could be reflected by the change of charge transfer resistance between electrolyte and electrode surface(Carvalho et al., 2018).

For LIG Micro-supercapacitors (MSCs) applications, the capacitance for energy storage between double layers of LIG formed the working principle here. There has been much research focusing MSCs derived from LIG induced from PI. In one reported study, LIG was generated on both sides of PI sheet first. Then, PI sheets with LIG on two side piled together to form multiple layers. Because of the porous structure of LIG, the MSCs displayed high capacitance and high conductivity(Wang et al., 2017). Besides, there is also another reported way in one previous study that using plasma treatment on MSCs to enhance MSCs's performance. When this treatment is applied, the capacitance of LIG MSCs can reach 18.3 mF cm^{-2} at a scan rate of 10 mV s^{-1} and 31.9 mF cm^{-2} at a current density of 0.05 mA cm^{-2} , which was better than most LIG-based MSCs in previous works(Cai et al., 2016).

For microfluidic devices and electrocatalysts applications based on LIG, LIG's, high chemical resistance and porous structure are LIG's advantages. Microfluidic device that can transfer organic fluids has been reported. Also, an efficient catalyst device that could directly produce H2 and O2 from water(Zhang et al., 2017).

In order to enhance LIG's performance in some applications, integrating LIG with compositions has been explored a lot as well. In one previous research, one research team tried combine LIG with pseudocapacitive materials via electrodeposition. Then, they successfully made LIG hybrid material such as LIG–MnO2, LIG–FeOOH, LIG–PANI. With these integrated materials, they fabricated micro-supercapacitors with energy density that was almost equal with daily-used lithium thin-film batteries(Li et al., 2016).

Different LIG precursor also has been explored a lot. At the beginning, materials including PI and polyetherimide (PEI) were considered to be standard precursor for high quality LIG production. However, with more research being reported, it has been confirmed that quality LIG also could be successfully obtained by using phenolic resin (PR) as the precursor(Z. C. Zhang et al., 2018), even from wood(Ye et al., 2017). Also, it was proved that wood with higher lignin content would lead to LIG with sheet resistance as low as 10 Ω/sq(Ye et al., 2017). Later, a new method called the defocused method has been found, which can nearly transfer any carbon-based substrates into LIG via CO2 laser in room conditions. The defocused method has significantly expanded the limited choices of precursor to almost any other carbon-based materials, providing LIG technology with potential to use more environmental-friendly and biodegradable precursor for high-quality LIG induing(Chyan et al., 2018).

LIG, because of its promising properties, such as excellent mechanical strength and high thermal stability, has aroused significant researchers' interests around the world. Especially, one previous study demonstrated that wood with a higher content of lignin could lead to better quality LIG (Ye et al., 2017). They attempted to emit a theory that the lignin's hexagonal microstructure might account for the quality of LIG induced on wood precursor. Research has shown that with this new laser method, the defocused method, almost any carbon-based material could be transferred into quality LIG(Chyan et al., 2018). However, among those work that had already produced LIG on various carbon-based precursors, there were usually two main issues in their work. First, in many results, the quality of LIG still have too much detective graphene. Second, LIG induced on many precursors like wood, or cloth, cannot be transferred easily to another substrate, which limited its application potential of being used in wearable devices. In many wearable device's applications, it is often required to transfer LIG from its precursor to a new substrate. In previous studies about on organic precursor, lignin-based precursor, some advantages have already been demonstrated in terms of two shortcomings talked above. In one of our group's previous studies, we have used kraft lignin to develop a lignin-based precursor. Then we have successfully made a flexible supercapacitor with LIG obtained from their lignin-based precursor(Mahmood et al., 2019). In this study, our prior research focused on synthesizing higher quality LIG from lignin and then further make it into wearable devices, where we used the LIG derived from lignin for physical sensing applications for the first time.

1.2. Goal and objectives

We used lignin to form a solid and water-soluble substrate first, making it possible for one-step laser writing to induce high-quality LIG with sheet resistance as low as 5 Ω per square. The LIG was then used to fabricate strain sensors, which was further tested on real body movements. The project has two specific aims described below.

Aim1: Develop a lignin-based precursor and characterize LIG derived from it.

It is our hypotheses that a higher concentration of lignin in the precursor will lead to LIG with higher conductivity and use of different elastomer formed solid films with different physical properties. We used different lignin to develop precursors. Then lignin was mixed with PVA to form a solid film. LIG was induced by direct laser writing on the lignin-based film. At last, by using specific instruments, the LIG was characterized from aspects including morphonology and electrical properties.

Aim 2: Fabricate strain sensors using lignin-derived LIG and evaluate sensing performance of LIG-based devices.

LIG on lignin-based precursors were transferred on a biocompatible silicon substrate by directly dissolving the precursor with water. Based on our preliminary data, different thicknesses of new substrate for LIG will influence device sensitivity. Spin coating will be applied to control the thickness of silicon substrate. LCR meter will measure the resistance change ($\Delta R/R0$). The sensitivity of the strain sensor was determined by the ratio between $\Delta R/R0$ and $\Delta C/C0$ under certain strains.

Chapter II Literature review

2.1 Introduction

Laser-induced graphene is a new material that is developed by direct laser writing on a carbon-based substrate. In previous studies, graphene was usually developed by using chemical vapor deposition and hydrothermal method(Chen et al., 2011). However, both methods require strict high-temperature conditions and complex steps, which cost a great deal and limit its application potential for large scale fabrications. In 2014, it was found that CO2 laser can directly generate laser-induced graphene (LIG) on polyimide film (PI). The induced LIG has many excellent chemicals, physical, and electronic properties such as chemical resistance, excellent thermal stability, and conductivity(Lin et al., 2014). This finding had greatly aroused enthusiasm for research in this field, from precursor development to LIG applications. Not only limited to materials like PI and polyetherimide (PEI), a new material called phenolic resin was also found suitable for LIG inducing (Z. C. Zhang et al., 2018). Later, there was emerging a new laser method called the defocused method, through which nearly all carbon-based precursors can be converted into graphene via direct laser writing. Besides CO2 infrared lasers, visible laser and ultraviolet laser have also been confirmed to be LIG inducers(Carvalho et al., 2018). Moreover, Scientists also tried to use LIG for various applications such as energy conversions---water splitting(Zhang et al., 2017), sensors for sound(Tao et al., 2017), strain and chemicals detection(Carvalho et al., 2018) and microfluidics devices(Tiliakos et al., 2016). We can see that there have already been many alternatives of controllable LIG development methods and numerous LIG-based applications. In this literature review, we will discuss

the LIG development from its start to its various applications and the greener precursors for LIG in the future.

2.2 Synthesis of LIG

In 2014, it was found that a porous structure could directly be obtained in ambient conditions using direct CO_2 laser writing(Lin et al., 2014). It just needs one-step laser writing on PI, and the pattern could be controlled by computer. It could be described in the following two steps. First, under ambient conditions, a PI film was placed under a CO_2 laser machine. Second, with computer-controlled laser scribing, the laser energy turned the substrate into a porous structure which was named laser-induced graphene (LIG). Moreover, researchers found that changing the laser energy, speed, and laser cycles could alter the graphene morphology. It was found that to initiate the carbonization process, radiation energy should be no less than ~5 J/cm^2(Lin et al., 2014). When this radiation energy >40 J/cm^2, LIG morphology would be changed from sheet texture to fibers(Duy et al., 2018). One research team developed a method to produce carbon nanotubes (CNTs) via repeated laser writing(Tiliakos et al., 2016). It was has been demonstrated that it is also possible to obtain LIG using an ultraviolet laser instead of a CO2 laser(Carvalho et al., 2018).

What we mentioned above are some parameters in laser setting. At the same time, there are many other studies focusing on utilizations of different substrate materials for LIG generation as well as how further to modify LIG to enhance its performance in applications. For the exploration of precursors, scientists found that many new precursors not just PI can be turned into LIG using CO2 laser. It had been reported that phenolic resin (PR) could be used as the precursor and produce LIG as well(Z. C. Zhang et al., 2018).

Later, a developed a method called defocused method could turn various carbon-based substrates into LIG using the CO2 laser in room conditions(Chyan et al., 2018). They used a technique called the defocused method. By changing the z-axis distance, the size of the laser spot in the substrate can be changed. The overlapping of the spots at the same position causes multiple lasing in just one pulse of the laser. Compared with the focused condition, it didn't cost extra time. One previous work has confirmed that wood with higher lignin content is more likely to generate high-quality graphene(Ye et al., 2017). With the focused laser in the previous study, inducing LIG from wood needs inert gases like Ar or H2 to prevent burning. With the adjusted defocused method, the burning issue could be avoided in ambient conditions. This method has expanded the potential to use more sustainable precursors for LIG. However, the main problem is that the quality of LIG induced on many carbon-based materials like wood is usually hard to control(Ye et al., 2017).

When many different precursor options can generate LIG with high quality, deposition of LIG, subsequently depositing functional materials on the LIG, is also a method that can enhance the LIG quality. For example, there was one method called electrodeposition(Li et al., 2016). Combining pseudocapacitive materials with LIG, LIG hybrid material like LIG–MnO2, LIG–FeOOH, LIG–PANI, had successfully been synthesized to fabricate micro-supercapacitors with an energy density like daily-used lithium thin-film batteries(Li et al., 2016).

2.3 Applications

With the rapid growth of LIG synthesis technologies, there are also various applications related to it coming out. Those applications can be roughly divided into the following categories: sensors, micro-supercapacitors, and microfluidic devices.

2.3.1 Sensor

For sensor applications, mainly there are two kinds of LIG-based sensors, chemical sensors, and mechanical sensors. The chemical LIG sensor's working mechanism usually depends on changes in electrical signals upon the specific binding of chemical substances to the LIG surface. In one previous study, an LIG electrode was used to detect chloramphenicol (CAP) via a biorecognition element. It was a 3-electrode system, which the researcher designed by using graphene from PI as working electrodes. The concentration of CAP could be reflexed by the change of resistance between the electrode surface and electrolyte(Tokonami et al., 2012). The study mentioned above is typical chemical sensors based on the specific binding approach. There also is another kind, a chemical sensor that are based on non-specific binding, like chemical redox reactions. Since non-specific binding sensors do not need extra elements like antibodies and aptamer, it usually costs less. In on previous study, direct laser engraving graphene (DLEG) and copper nanotubes (CuNCs) were used to create a disposable glucose sensor. In this system, all three electrodes were made by DLEG hybrids. It meant this device was very low-cost and could be fabricated quickly. However, the significant limitation associated with their study was that all the experiments were conducted in an in-vitro environment(Tokonami et al., 2012).

The LIG mechanic sensors usually rely on the piezoresistive effect. One team reported a low-cost LIG artificial throat by using LIG induced from PI. This device could generate and detect sounds based on the piezoelectric effect and inverse piezoelectric effect. The proper regeneration was based on establishing a database and machine learning because different movements had unique characteristic waveforms(Wang et al., 2017). Similarly,

depending on where deformation comes from, LIG mechanical sensors could also be used to detect many other biological activities like body movements such as heartbeat or pressure. Another team used LIG and carbon nanotube to fabricate a strain sensor. The device can withstand up to 100% strain, and its gauge factor could be as high as 20,000(Rahimi et al., 2015).

2.3.2 Micro-supercapacitors

LIG-based micro-supercapacitors (MSCs) were usually based on the capacitive double layer of LIG. 3D micro-supercapacitors based on LIG induced from PI sheets had already been demonstrated. In this work, LIG was generated on just one side or two sides of the PI sheet. These LIG on PI at two sides were prepared for the fabrication of multiple-layer supercapacitor. In the first step, to enhance its electrical contacts, silver paint was applied on the connection areas of each electrode. Finally, one LIG-PI substrate was combined with a second one, with PVA/H2SO4 dropped between each layer. Under different scan rates and current densities, the LIG-based MSCs show high capacitance, which is due to the porous structure and high conductivity of LIG(Wang et al., 2017). In addition to the method mentioned above that used innovatively physical design to realize high capacitance, LIG MSCs were integrated with compositions to improve its capacitance as well. For example, in one previous study, plasma treatment had been adopted to enhance LIG-based MSCs capacity performance. It had been reported that after plasma treatment to the MSCs for 100s, the improved capacitance reached 18.3 mF cm−2 at a scan rate of 10 mV s−1 and 31.9 mF cm−2 at a current density of 0.05 mA cm−2. The optimized capacitance of the LIG-based MSCs was better than most LIG-based MSCs in previous works (Cai et al., 2016).

2.3.3 Microfluidic Devices

LIG is also porous and chemical-resistant structure. Both features could be made full use of in microfluidic devices as the permeable channels. One team used BCP to develop LIG-based microfluidic channels via laser writing. The device contains a groove for flowing fluid formed by resol etching, a porous tunnel formed by BCP laser irradiation at the bottom of the track, and a polydimethylsiloxane (PDMS) on the top of the device seals. This microfluidic device is capable of transporting organic solutions(Tan et al., 2015).

2.3.4 Electrocatalysts

The porous structure of LIG also enables it to be an efficient catalyst in various chemical reactions. In one previous study, one team fabricated three catalytic LIG electrodes (LIG-Pt, LIG-Co-P, LIG-NiFe) by *in situ* doping or electrochemical deposition on LIG induced from cheap plastic film. This device was used to generate both H2 and O2 from water and showed highly efficient catalytic activity(Zhang et al., 2017).

2.4 Conclusions

Since the discovery of LIG in 2014(Lin et al., 2014), the synthesis technology of LIG has been significantly improved and applications derived from LIG are consistently coming out. As we discussed above, the LIG could be applied to many applications such as chemical and mechanical sensors, micro-supercapacitors, microfluidic devices, and electrocatalysts.

For chemical and mechanical sensor applications, they often show high sensitivity and high stability(Rahimi et al., 2015; Tehrani & Bavarian, 2016; Tokonami et al., 2012). However, sensors with high sensitivity usually can only detect a single parameter. For future needs, a multifunctional and wirelessly device that can detect in real-time is more

favorable. Additionally, there is a need for higher sensitive electrochemical sensors based on the LIG electrode. Aspects such as enhancing the surface-functionality and improving the electrical property by using novel composite materials should be considered. For sensors monitoring human health, biocompatibility and safety are also significant factors that should be taken into account. For MSCs application, although electrical double-layer capacitors have been successfully fabricated in many previous studies, there are not many reports that are using the pseudocapacitance principle to develop supercapacitors with larger energy densities(Fleischmann et al., 2020). For microfluidic devices and electrocatalysts applications, more efforts should be made to improve the mechanical stability of LIG porous structures.

As discussed above, PI is the most widely used precursor for LIG. This is because the LIG induced from PI has more excellent chemical and mechanical properties than the other. With the rapid growth of the LIG application, we should raise our concern about the electronic waste issue(Ye et al., 2019). PI has excellent features like excellent thermal, chemical, mechanical stability, and low cost, but it is difficult to recycle and unsustainable. With many reports of using other carbon-based materials for LIG(Chyan et al., 2018; Ye et al., 2017) and improved laser technique such as defocused method(Chyan et al., 2018), biodegradable and biocompatible LIG applications from more environmentally-friendly precursors will be developed in the future.

Chapter III Lignin-derived Laser Induced Graphene for Ultrasensitive Sensing

3.1 Abstract

Recently laser-induced graphene (LIG) has attracted much attention due to its promising features that can be used in numerous applications. It has been confirmed that many materials can be used for LIG generation, like polyimide film(Lin et al., 2014), polyetherimide, phenolic resin, even wood, cloth, food, or any carbon-based materials(Chyan et al., 2018). Among those precursors, a raw material that is environment-friendly and can generate high-quality LIG simultaneously is needed. Lignin is a nationally occurring aromatic polymer and usually an industrial waste from pulping and biorefinery industries. With aromatic structure, the potential of lignin being used as a LIG precursor has already been proved in some previous study(Mahmood et al., 2020; W. L. Zhang et al., 2018). Here, we demonstrated how we used a lignin-based precursor to generate high-quality LIG and further used the LIG to fabricate ultra-sensitive strain sensors by transferring it onto dragon skin. Within the strain range of 0%~9%, the gauge factor of our strain sensor is about 166. Within the strain range of 9%~14%, the gauge factor is up to 924. Furthermore, the repeatability and durability of our strain sensor have been tested by 4000 cycles under 4% strain applied. At last, our ultrasensitive strain sensor has been further used for detection for speaking, pulses, eye movement, even sound passing in the air.

3.2 Introduction

Laser-induced graphene is a 3D structure that is developed by direct laser writing on a carbon-based substrate. In 2014, It was found that CO2 laser can directly generate 3D

Laser-induced graphene (LIG) on commercial polyimide film (PI). LIG has many excellent chemical, physical, and electronic properties such as chemical resistance, high thermal stability, and high conductivity(Lin et al., 2014). This finding had incredibly aroused enthusiasm for research in the field of LIG, from precursor development to its applications. Not only limited to materials like PI and polyetherimide (PEI). In previous work, phenolic resin had also been converted into LIG through laser writing(Z. C. Zhang et al., 2018). Later, a new laser method called the defocus method was reported, through which nearly all carbon precursors can be converted into graphene in ambient atmospheres(Chyan et al., 2018). Besides CO2 infrared lasers, visible laser(Z. C. Zhang et al., 2018) and ultraviolet lasers(Carvalho et al., 2018) have also been used to synthesize LIG. Scientists focused on converting varied materials into LIG and used it for numerous applications, such as supercapacitors(Lamberti et al., 2016) for energy storage, sensors for sound(Tao et al., 2017), strain(Chhetry et al., 2019), chemicals sensor(Cheng et al., 2016) and microfluidics device(Griesche et al., 2021). We can see that there have already been many controllable LIG development methods as well as many applications derived from it.

LIG has aroused tremendous research interests due to its intriguing properties, such as high thermal stability and excellent conductivity. One study has revealed that with one advanced laser method called the defocused method, almost any carbon-based material could be turned into quality LIG(Chyan et al., 2018). Especially it was confirmed that wood with higher lignin content has been proved to be favorable for LIG formation(Ye et al., 2017). In another previous studies, the LIG induced on lignin-based precursors has shown its promising properties and further has been utilized into supercapacitors for energy storage. Compared with LIG indued on other carbon-based materials, like wood or paper,

LIG indued on lignin-based precursor is more favorable for the transfer process required by wearable devices. Still, there is not much exploration of LIG induced from lignin-based precursors on its utilizations into wearable devices, which are already realized by LIG induced from PI, etc.

Strain sensor usually plays an essential role in human health monitoring. Many previous studies have successfully made strains sensors with an excellent performance by using LIG(Carvalho et al., 2018; Cheng et al., 2015; Chhetry et al., 2019; Jeong et al., 2019; Park et al., 2015; Tao et al., 2017; Wang et al., 2015). Those strain sensors have been used for many different detections of human motion monitoring or gesture capturing. Polyimides are usually standard precursors used for these sensors' fabrications. Without any pretreatments to precursors or modifications on LIG, the gauge factors of strain sensors developed from polyimides are usually below 200, which is not low but can be higher. In strain sensor study, more significant electrical signals change caused by minor deformation of the sensor itself is a standard of its sensitivity. In other word, the higher gauge factor, the better. Also, the features of lower cost, the easier process of fabrication, and good stability all would be of the primary considerations.

Our research demonstrated how we developed a kraft-lignin precursor that can be used for high-quality LIG generation through laser writing. Then, we explored LIG derived from lignin for the fabrication of an ultra-sensitive strain sensor for the first time. Here, the cost for raw material is low as kraft lignin is usually an industrial waste and widely exists worldwide. Also, the fabrication process is straightforward. No additional pretreatment to precursors or modifications on LIG is needed.

3.2 Method

3.2.1 Development of lignin-based precursor

Polyvinyl alcohol (PVA) was first dissolved in deionized water by continuous stirring at 90 °C for 40 mins, PVA: DI water=1: 10. Then, 0.5, 1, and 1.5g kraft lignin were dissolved in 10g 2% NaOH solution, respectively. Then 10g PVA solution was poured into each dissolved lignin solution. Stir the whole solution until a black-brown homogeneous mixture was obtained. Then, the black-brown mixture was transferred onto a plastic dish and then put into an incubator with a temperature of 35 ℃ and humidity of 15%~50% for around 30 hours. After drying, the precursor was taken out of Petri dishes and attached to the glass film using adhesive tape for laser writing.

3.2.2 Synthesis of LIG

For the synthesis of LIG, a 30 W and 10.6 μm CO_2 laser (Universal Laser Systems VLS3.50 Laser Cutter/Engraver) was used under ambient conditions for LIG formation. One thousand pulses per inch (PPI), 10% speed, and an extra 2mm Z-axis distance were fixed for all laser processes. Different laser powers 20%, 30%, 40% were applied on each precursor in turn. The area scanned by laser is a rectangle with a length of 30 mm and a width of 5 mm.

3.2.3 Strain sensor's fabrication

The LIG we used to fabricate sensors was from a 1g 30% sample. First, the dragon skin prepolymer mixture (part A / Part B = 1:1, w/w) was poured over LIG samples. Spin coater (Model WS-650MZ-23NPPB) was used here, with a spin speed of 3000 round/min, accelerated speed of 500. Then, the sample was put in an oven for solidification at 35 ℃

for 30mins. After solidification, the whole sample was put into the DI water which helped LIG fall off from the lignin precursor. Then, the obtained LIG on dragon skin was put into an oven at 35 ℃ again for 20-mins drying. After drying, two copper wires were adhered to on both ends of the transferred LIG by using the conductive epoxy. After final air drying for the epoxy, the sensor fabrication was completed.

3.2.4 Characterizations of LIG before and after transfer

For LIG before the transfer, the sheet resistance of LIG samples was measured by Lucas Labs - Pro-4 Four Point Resistivity Systems. For both LIG before and after the transfer, the surface morphology of the LIG was observed by using Scanning Electron Microscope (SEM). Raman analysis for all samples was done via Raman spectroscopy. All measurements of resistance change were done by an LCR meter.

3.3 Results and discussion

a.

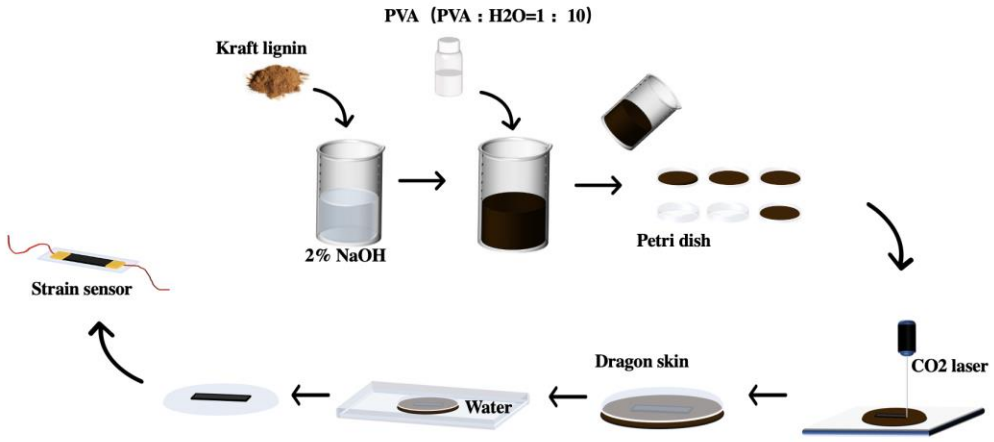

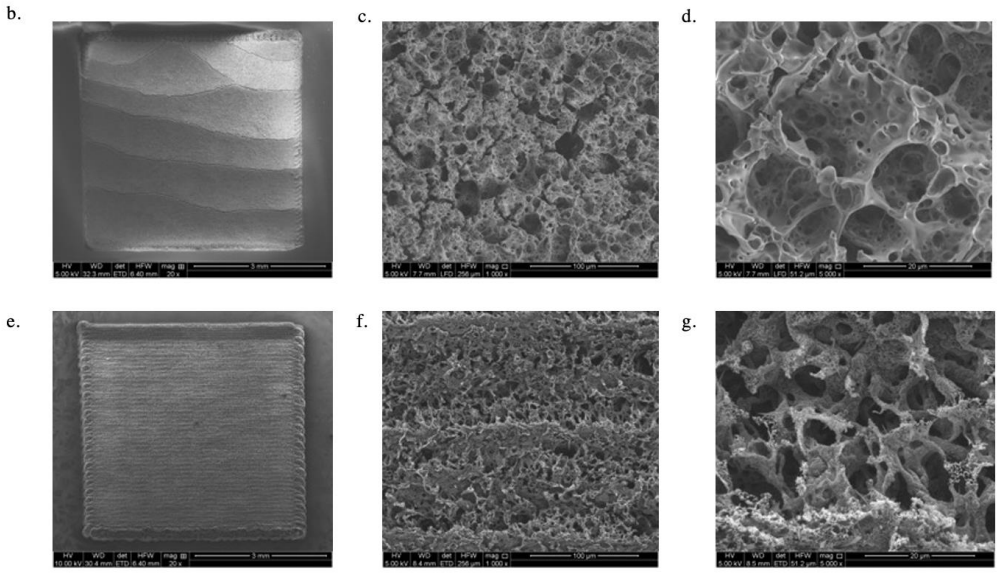

Figure 1. (a) schematic illustration of the whole experiment methods. (b)~(d) SEM images of LIG sample1g 30% before and after transfer. (e)~(g) SEM images of LIG sample1g 30% after transfer. (b)&(e) scale bar 3mm. (c)&(e) scale bar 100 μm. (d)&(g) scale bar 20 μm

3.3.1 Fabrication and characterization

Figure 1a illustrates the whole experiment method, including the development of lignin-based precursor, synthesis of LIG, and strain sensor fabrication. The first step was to develop a lignin-based precursor. Here, to further explore how the concentration of lignin in precursor affected the quality of LIG under the same laser condition, we prepared lignin solutions at three different concentrations, 0.5, 1, 1.5g, in the same dissolving solution (10g 2% NaOH + 10g PVA (PVA: H2O=1:10). After drying these precursors, three different laser settings had been applied, 20%, 30%, and 40% laser power. Here, Laser speed 10%, pulse per inch (PPI), and z-axis distance 2mm were fixed and applied to

all samples. Then, sheet resistance measurements and Raman analysis had been done on all samples. X-ray photoelectron spectroscopy (XPS) and measurement of Scanning Electron Microscope (SEM) had only been done to LIG on sample 1g 30%, including before and after transferring condition since based on its Raman spectrum, this LIG has the best graphene-like properties, and we used this LIG in the following sensor's fabrication. In the fabrication of strain sensors, first, the LIG on sample 1g 30% would be transferred to dragon skin under the control of spin coating. Second, after transferring LIG to the dragon skin, a conductive epoxy paste was used to connect copper wires at two ends of LIG. More detailed fabrications details could be found in the Method section. In Figure 1b, the SEM images of LIG sample 1g 30% before and after being transferred to dragon skin have been shown in figure 1b. We did SEM analysis only on LIG sample 1g 30% here because LIG sample 1g 30% was what we used to fabricate the strain sensor in the following steps. The clear lines can be observed in SEM images of LIG sample 1g 30% before the transfer, which was formed orderly along the traces of CO2 laser. In SEM images of LIG sample 1g 30% after the transfer, no laser trace can be seen, and the pore size is more prominent while the pore surface looks smoother.

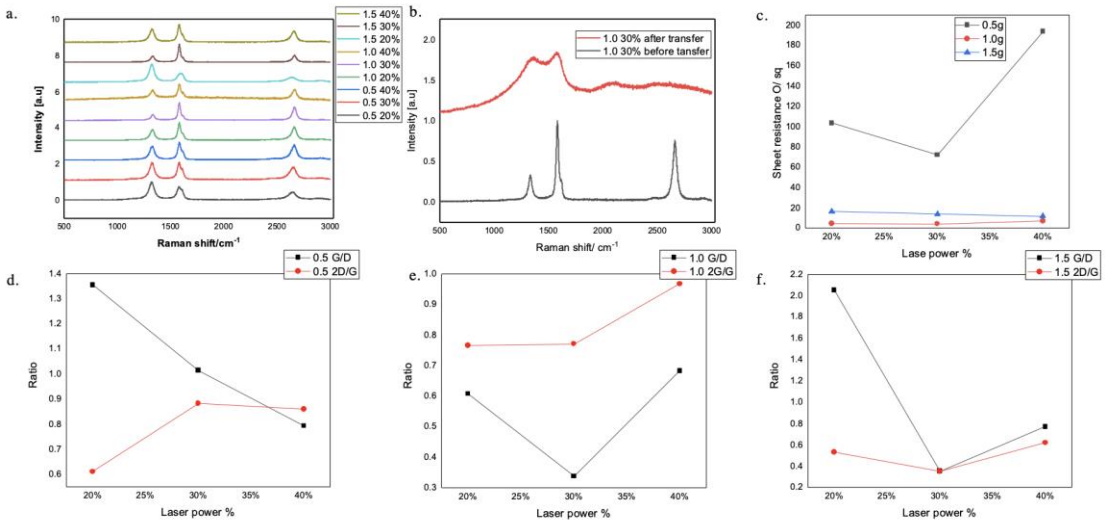

Figure 2 Characteristics of Raman, sheet resistance. (a). Raman spectra of LIG induced on the different samples with different laser power. (b). Raman spectra of LIG induced on the sample "1g 30%", the red line is the Raman spectra after the transfer, the black line is the Raman spectra before transfer. (c)The sheet resistance of LIG is induced on different precursors by different laser power. (d). The ratio of D peak versus G peak and the ratio of 2D peak versus G peak on LIG induced from precursor "0.5 20%", "0.5 30%" and “0.5 40%”. (e). The ratio of D peak versus G peak and the ratio of 2D peak versus G peak on LIG induced from precursor "1.0 20%", "1.0 30%" and “1.0 40%”. (f) The ratio of D peak versus G peak and the ratio of 2D peak versus G peak on LIG induced from precursor "1.5 20%", "1.5 30%" and “1.5 40%”.

Raman spectrometer was used for the analysis of the chemical structure of LIG from our different precursors. Here we had nine different precursors. In the precursor-making step, we made three different precursors that have different lignin concentrations. The laser power (20%, 30%, 40%) has been done on each sample in the laser writing part. Laser speed (10%), power per inch (1000), and Z-distance(3.5mm) are applied to all samples. In all of Raman spectrums, the D-peak, G-peak, and 2D-peak can be observed. Here, the D-peak can be observed at 1350 cm^{-1} indicating defective graphene. The G-peak can be observed at 1550 cm^{-1}, proving a carbon bond stretching in both the ring structure and the chain structure. The 2-D peak at 2700 cm^{-1} shows the degree of how well the substrate has been graphitized. Then, the quality of LIG indued on different precursors will be further evaluated by the ID/IG and I 2D/ IG, shown in Figures c, d, and e. Figure 3d shows the ID/IG and I 2D/ IG of sample 0.5g. With laser power increasing, the ID/IG kept going

lower while the 2D/ IG did not keep increasing from laser power 30% to 40%. However, even so, we still can see that in sample 0.5g, a precursor with lower lignin concentration, quality LIG cannot be induced well. Figure 3e shows the ID/IG and I 2D/ IG of sample 1.0g. Compared to different laser conditions, we can tell that the laser power that can lead to the best quality LIG is 30% instead of 20% or 40%. Figure 3e shows the ID/IG and I 2D/ IG of sample 1.5g. At the same low laser power of 20%, we can see that the ID/IG was 2.05 while 2D/ IG is 0.53, indicating no quality LIG induced.

Based on the results, we can see that at a laser power of 30% on precursor-1.0, the best LIG can be generated with the highest 2-D peak and lowest D-peak. We found that higher lignin concentration in the lignin-based precursor leads to better quality LIG. For example, on the precursor with a lower lignin concentration, quality LIG cannot be well induced. On the precursor with a higher lignin concentration, the LIG induced at different laser power is still not the best. Only a particular concentration in lignin precursor (1g kraft lignin+0.2g NaOH+ ~1g PVA) at a particular power could lead to the best quality LIG.

In summary, lignin concentration should be within a specific range, if we wanted to induce quality LIG on lignin-based precursors just by low-power and one-time laser wiring. Here, a possible explanation for the observations shown above was that quality LIG induced from lignin-based precursor benefited from the original structure of kraft lignin, the structure of multiple benzene rings. When lignin is dissolved and mixed with PVA, only at a particular concentration can lignin be spread out more uniformly. Then, laser writing could better turn the kraft lignin structure into a graphene-like structure.

We primarily did the Raman analysis on a 1.0 30% sample after the transfer (Figure 3b). Here, we can see that the Raman spectrum of the 1.0 30% sample after the transfer

did not correspond to the three peaks that LIG has. The 2-D peak was gone, and the ID/IG here tells us it was just activated carbons that had not been well induced.(Ferrari & Robertson, 2000) Combined with the SEM data, we can tell the bottom side of the sample induced on precursor didn't have good graphene-like structure that could be found in similar previous studies. For example, in one previous study, it was found that for LIG induced on wood by relatively lower laser power, the 2D peak was not prevalent, which indicated that with insufficient laser energy, the lasered lignin precursor would be just converted into activated carbon instead of activated LIG(Ye et al., 2017). In another relevant study, it was also mentioned that higher laser power would better initiate the grapheneization process and lead to better quality LIG(Lin et al., 2014). Thus, in our research, the reason why the characterizations of the bottom side sample were showing that the structure had been well induced, was because the energy was not sufficient, which had been mostly absorbed by surface of the lignin precursor. When the laser has reached a deeper layer, the decreased laser energy could not initiate the grapheneization process.

Figure 3c had shown the sheet resistance of LIG induced on different precursors by different laser power. We can see that precursors with lower lignin concentrations cannot generate LIG with low sheet resistance when the lignin concentration had not reached a certain level. For example, on precursor with lignin concentration of 1.0g 1.5g, all the LIG induced under power 20%, 30%, and 40% have low sheet resistance, while LIG induced on precursor with 0.5g lignin could not generate LIG with low sheet resistance. On precursor with 1g lignin, the LIG induced under power 30% had the lowest sheet resistance, 4.05 Ω/sq. Sheet resistance is one of standards that reflect the structure' grapheneization. Notably, we can see that the sheet resistance of LIG induced on precursors with 1g lignin

is lower than LIG induced precursor with 1.5g lignin. This result indicates that a higher lignin concentration will not always lead to better quality LIG and that a specific concentration of lignin in precursor will lead to the best quality LIG. Combining Raman results and SEM above, we would have a similar interpretation that precursors with a lower concentration of lignin are not suitable for generating high-quality LIG, and that only with a certain concentration of lignin could the precursor generate high quality LIG. Compared with LIG induced on wood that previously explained due to the cross-linked lignocellulose structure (Ye et al., 2017), our optimized LIG induced on lignin precursor has better quality, which has lower sheet resistance (4.05 Ω/sq), less defective graphene, and better-grapheneization structure. Most importantly, the LIG induced on our lignin-based precursor is favorable for being transferred to new substrates, which enable itself can be used in more applications, like many soft wearable devices.

3.3.2 Sensing stretches and sensing of vibrations

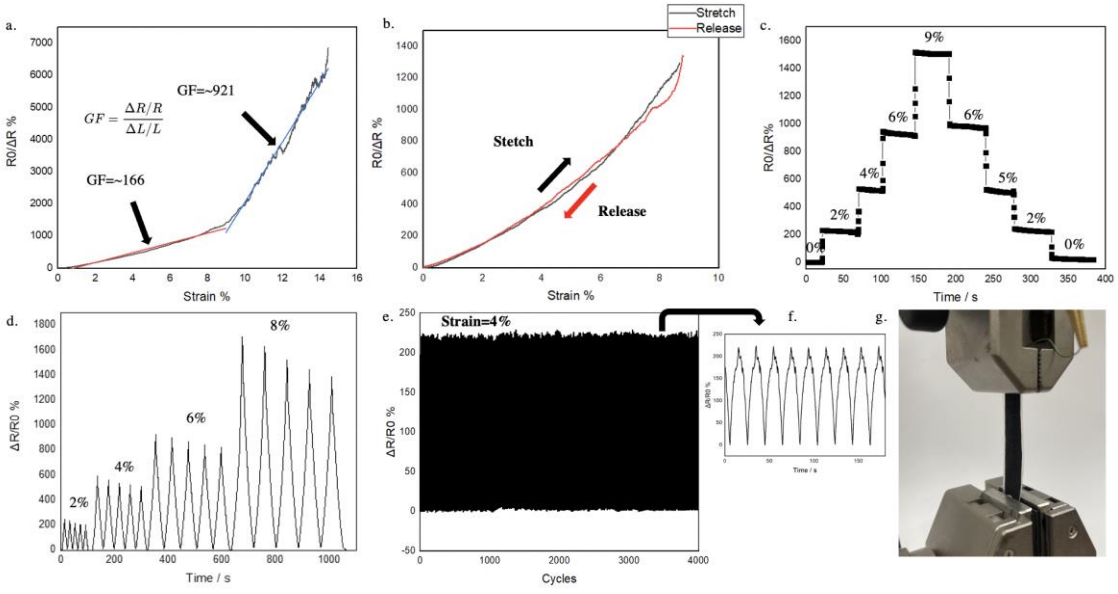

Figure 3. The sensor's sensitivity to strains. (a) the relative resistance change of strain sensor when strains are applied linearly. (b) the relative resistance change of strain sensor

when it was stretched (black line)and released (red line), under the strain of 8%. (c) the relative resistance change of strain sensor. (d) the dynamic relative resistance change of strain sensor under different strains applied, 2%, 4%, 6%, 9%. (e) Stability of the strain sensor at 4% strain for 4000 cycles. (f) Nine times cycles during stability test. (g) Schematic diagram of strain sensor stretched.

Our strain sensor had a length of 38.0 mm, a width of 8.5mm, and was embedded in dragoon skin substrate with a thickness of 0.25mm. This chapter measured our strain sensor's sensitivity in terms of two external stimuli, strains, and vibrations. As shown in Figure 4g, where the strains sensor was stretched, we could see the increasing gap distance while strains applied increased. Like strain sensors based on the cracked structure was precious research (Kang et al., 2014; Tolvanen et al., 2018), our strains sensor is ultrasensitive to strains as well, because of the minimal cracks under strain. The strain's sensitivity to increasing strain (from 0% to 14%) had been shown in Figure 4a. We could see that the device went through two different stages with increasing strain. Within the strain range of 0%~9%, the gauge factor here was about 166. Within the strain range of 9%~14%, the gauge factor here was about 924. It was not hard to understand, since many precious studies had the similar observations. It was because that when larger strains applied had reached a certain level, the crack between graphene flakes would lead to a new junction resistance connection. That explained why there was a turning point. When the crack was too large, the electrical connection between the two ends of the strain sensor would be broken and become non-conductive. For our strain sensor, the maximum strain that could be applied was ~ 14%. The stretch speed here is 0.2mm/min. One of the reasons why the maximum strain applied could not exceed 14% was because we used the thinnest

substrate here, which only have the thickness of 0.25mm. Notable, we could see that in the first stage, when the strain is below 9%, the signal was more stable and had a better linear relationship. Figure 4b showed the reversibility of our strain sensor under 9% strain. Good reversibility could be observed here. Figure 4c showed the signal stability when different strains were applied. Respectively, different strains, 2%, 4%, 6%, 9%, had been applied to our strain sensor. For each applied strain, each apply would remain for around 50s. We can see that the signal of relative resistance change was stable when a specific strain was applied. Based on the asymmetric relative resistance change pattern, we could tell our strain sensor's sensitivity to a certain stretching degree is repeatable and stable as well.

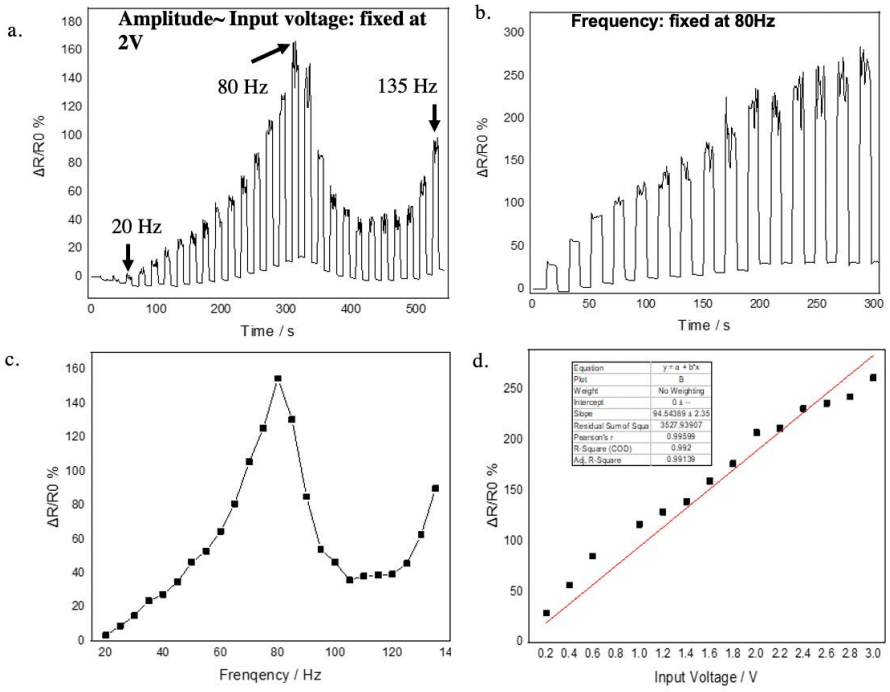

Figure 4. The strain sensor's sensitivity to vibrations (a) the relative resistance changes of strain sensor when different frequencies 5Hz—135Hz were applied in 500s, amplitude fixed at 2V. (b) the relative resistance changes of strain sensor when different amplitudes 0.2V—3Vwere applied in 300s, frequency fixed at 80Hz. (c) averaging the peak value in

figure 4a, clearer relative resistance changes under different frequencies applied are shown. (d). averaging the peak value in figure 4b, a clearer relative resistance changes under different amplitudes applied is shown.

Because of our strain sensor's ultra-sensitivity to strains, we further planned to measure its sensitivity to vibrations as well, which is another form of tiny deformations. To Further determine our strain sensor's sensitivity to vibrations, here, we used a shaker (b&k v203) to vibrate our sensor with different frequencies and amplitude and to consistently measure its resistance at the same time via LCR meter. In Figure 4a, we set the amplitude at 2V, starting the frequency at 5Hz, then 10 Hz, 15 Hz, 20Hz….135Hz. In each vibration with a certain frequency, we kept the sample vibrating for 10s and then let it rest for another 10s; we could see that our strain sensor's relative resistance change was different at different frequencies. Figure 4c shows that at a frequency of 85 Hz, the most significant relative resistance change can be observed. The resistance between the two ends of our strain sensor was related to the degree of deformation so that we could tell 85 Hz is the resident frequency of the whole sample. In Figure 4b, we fixed the frequency of 85 Hz and measured the strain sensor's relative resistance change at different amplitudes, starting at 0.2V, then 0.4V, 0.6V…3V. In vibration with a different amplitude, we kept the sample vibrating for 10s. In Figure 4d, with the amplitudes linearly increasing, we could see the resistance between two ends of our strain sensor was linearly increasing too. On the one hand, the results showed that our strain sensor had a sensitive and stable response even to external stimulations like vibrations. On the other hand, it also explained why it had excellent performance working as a speaking detector in our next chapter, since human speaking frequency is ranging from 50 Hz to 300hz.

3.3.3 Speaking sensor

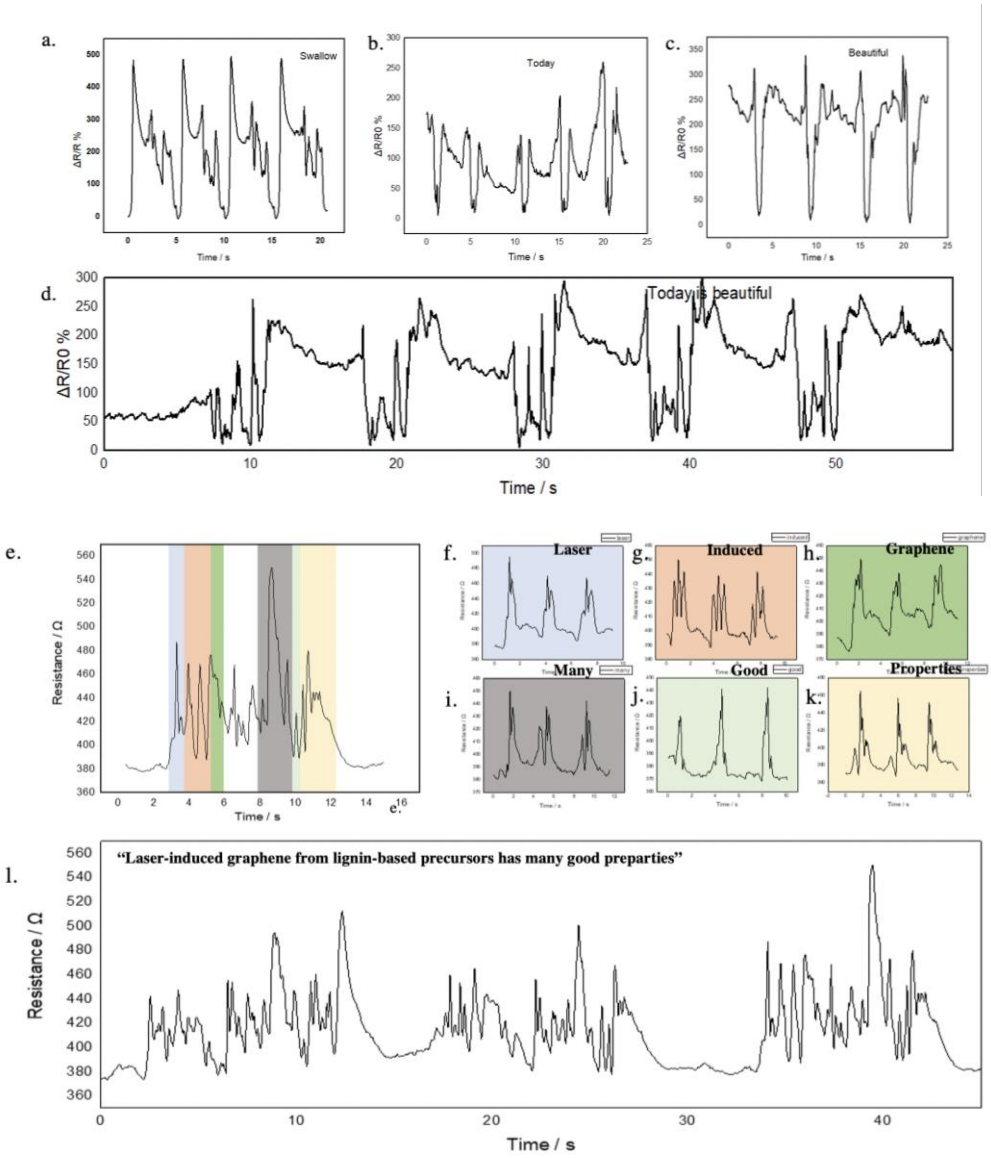

Figure 5. Strain sensor working on monitoring small human body motions. (a) the resistance signal pattern when the sensor is detecting swallow. (b)~(d) The relative resistance change in detection of speaking "beautiful," "today," and "today is beautiful." (e) the resistance signal pattern when the tester speaks "Laser-induced graphene from lignin-based precursor has many good properties" for one time. (f) the resistance signal pattern when the tester was speaking "laser." (g) the resistance signal pattern when the

tester was speaking "induced." (h) the resistance signal pattern when the tester was speaking "graphene." (i) the resistance signal pattern when the tester was speaking "many." () the resistance signal pattern when the tester was speaking "good." (j) the resistance signal pattern when the tester was speaking "properties." (i) the resistance signal pattern when the tester speaks "Laser-induced graphene from lignin-based precursor has many good properties" for three-time.

To further explore our strain sensor's potential in monitoring small human motion, our strain sensor had been tested for detecting human throat movement, speaking, eyeball movement, pulse. First, the strain sensor was attached to a person's throat. In Figure 5a, the person was asked to do the movement of swallowing four times. We could see the signal of relative resistance change when the signal was very repeatable and stable. Second, the tester was asked to say the words "today," "beautiful," "today is beautiful.". Figure 5b showed the resistance change pattern when the tester was saying "today" 5 times. Figure 5c showed the resistance change pattern when the tester was saying "beautiful" four times. In Figure 5d, the tester was asked to say "today is beautiful" 5 times. What's more, to further identify our stains sensor's sensitivity and accuracy in detecting human speaking, detecting test for longer sentences was done. In Figure 5e, the tester was asked to say, "laser-induced graphene induced from lignin-based precursor has many good properties." Still, the signal was repeatable and stable. In Figure 5f~k, the resistance change pattern was shown when the tester said words three times, respectively. In Figure 5I, the teste repeated the longer sentences, "laser-induced graphene induced from lignin-based precursor had many good properties" 3 times. We could see that no matter the tester said the word respectively or together in a completed sentence, short or long sentence, the unique and repeatable signal

of the resistance change pattern can be obverted. As our results compared with some similar previous study(Cheng et al., 2015; Park et al., 2015; Wang et al., 2015), we could see that our strain sensor has good repeatability and reliability for detecting the minor movement of a human's throat.

3.3.4 Pulse Wave, Eyeball Monitoring and detecting sound in the air

a.

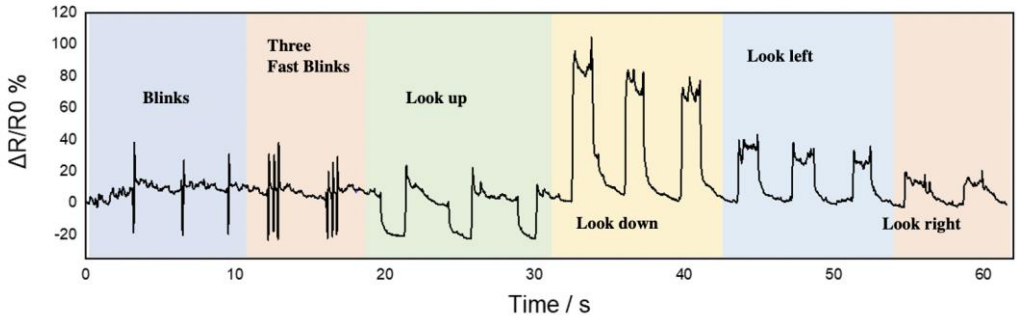

b.

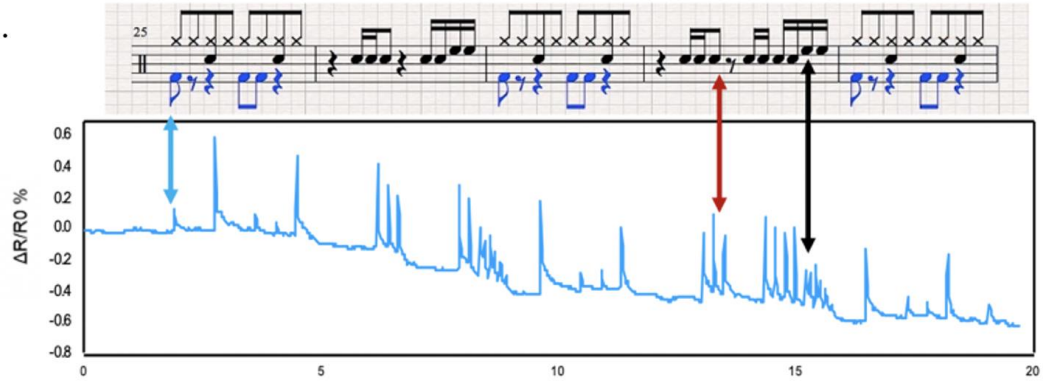

c.

d.

e.

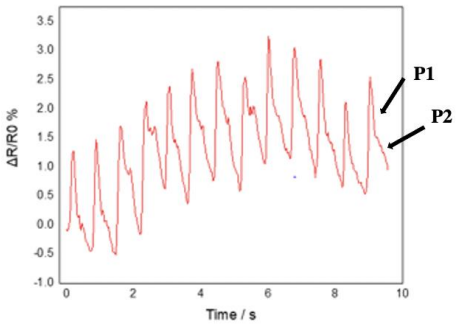

Figure 6 Strain sensor working on monitoring eyeball movement and pulses, detecting sound in the air. (a) the resistance signal pattern when the sensor is monitoring eyeball movements. (b) the resistance signal pattern when the sensor is detecting sound passing in the air. (c) Schematic diagram of sound in the air detection. (d) Schematic diagram of pulses detection. (e) the resistance signal pattern during pulses detection.

Based on our strain sensor's ultra-sensitivity to strain, we also further tested its performance in detecting human eye movements. First, in this test, we attached the sensor at the lower part of the tester's eye. Then, the tester was asked to do an eye blink, three fast eye blinks, looking up, looking down, looking left, and looking right at last. We can see that no matter for single eye blinks or fast eye blinks, our strain sensor could give instant and precise feedback. What is more, our strain sensor also has unique, stable, and repeatable signal pattern**s** towards different eye movement directions for the detection of eyeball moving directions. The working mechanism of our strain sensor here was the same. The eye movements are controlled by the muscle around. Also, the same eye movement has the same muscle controls. Figure 6a showed that our strain sensor generated a quick, stable, and repeatable signal of the relative resistance change during the same eye movements. Although the muscle controlling the eye had tiny movements when different eye movements were performed, our stain sensor could still detect the difference stably and accurately. The ultra-sensitivity of our strains sensor or minus deformation had been confirmed again. Also, compared with current real-time eyeball movement sensors(Al-Rahayfeh & Faezipour, 2013; Mishra et al., 2020), the method our strain sensor offering to monitor real-time eye movement detection is much easier.

Human pulse is also a critical factor in human body health monitoring. In figure 6d, we used our strain sensor to detect human pulses. In pulse detection, it is always an urgent need to distinguish the time delay between percussion wave(P1) and tidal wave(P2) related to one person's cardiovascular health(Yang et al., 2017). In our results, our strain sensor had successfully detected the percussion wave (P1) and tidal wave (P2), which had been pointed out in Figure 6e. This result showed the promising potential of our strain sensor for cardiovascular health monitoring.

We also tested our strain sensor to detect sound waves passing in the air for even tinier deformation detection. In Figure 6c, we put a loudspeaker 3 cm away in front of our strain sensor while the strain sensor was placing vertically. Then, a part of the music of drumbeats was played at 90 dB. Based on the result, three different sounds of drumbeats had been recognized successfully by our strains sensor. Figure 6a has displayed the relative resistance changes corresponding to three different drumbeats sounds. Even though the deformation caused by the sound wave in the air was minimal, our strain sensor was still able to detect them and had generated unique signal patterns for different beat sounds. This result had confirmed again that our strain sensor made of LIG induced from a lignin-based sensor has an excellent performance in detecting very tiny deformations.

Chapter IV Conclusions and Suggestions for Future Work

In summary, we have successfully improved the quality of LIG induced from lignin-based precursor and fabricated an ultra-sensitive strain sensor. The best LIG with the lowest D-peak and highest 2D-peak was induced from the sample "1g kraft lignin+ 0.2g NaOH+ 1g PVA 30%". After we transferred the LIG onto a dragon skin film, we made it into a strain sensor. Based on the result above, our strain sensor has an excellent performance in detecting small deformations. When strains are between 0%~9%, the gauge factor is around 166. When strains are between 9%~14%, the gauge factor is around 924. In both stages, a good linear relationship between the relative resistance changes and strains can be observed. Meanwhile, we also tested our strain senor's sensitivity to vibrations. Here, vibrations include two parameters frequency and amplitudes. Our strain sensor has successfully responded to vibrations with different frequencies and amplitudes. Moreover, to further verify our strain sensor's potential in monitoring human body movement, especially in small deformations, we had further tested our strain sensor in detecting human speaking, pulses, eyeball movements, and even sound passing in the air. In all the tests, our strain sensor has shown good stability and repeatability, generating characteristic signal patterns towards different deformations caused by different external stimuli. The results indicate the excellent sensing performance our strain sensor has. It is also indicating the potential of LIG induced from the lignin-based precursor. In this study we developed a simple, low-cost, repeatable method to make a lignin-based precursor and use the quality LIG induced from it to fabricate a strain sensor. Our work further explored the promising potential of lignin serving as LIG precursor.

As lignin is the most aromatic polymers in nature, the potential of lignin has not been fully explored so far, including its applications related to LIG. In the future study of LIG's applications, the multifunctional wearable device will be one of the hot spots in this research field. The platform of a multifunctional wearable device derived from lignin-based LIG can be envisioned, featuring cost effectiveness, high sensitivity and accuracy, being self-powered and durable, and biocompatibility. As LIG is the core part in any application, the quality and features of LIG will affect the device's performance. Although it has been confirmed that many materials can be used as LIG precursor, there is some difference of quality and features between LIG generated by different precursor or laser conditions. Lignin is emerging as a promising precursor for LIG production. The cost-effective, durable, flexible lignin-based precursor that allow quick transferring process at the same time will also enable us to explore more applications based on it.

Reference

Al-Rahayfeh, A., & Faezipour, M. (2013). Eye Tracking and Head Movement Detection: A State-of-Art Survey. *IEEE J Transl Eng Health Med*, *1*, 2100212. https://doi.org/10.1109/JTEHM.2013.2289879

Cai, J. G., Lv, C., & Watanabe, A. (2016). Cost-effective fabrication of high-performance flexible all-solid-state carbon micro-supercapacitors by blue-violet laser direct writing and further surface treatment. *Journal of Materials Chemistry A*, *4*(5), 1671-1679. https://doi.org/10.1039/c5ta09450j

Carvalho, A. F., Fernandes, A. J. S., Leitão, C., Deuermeier, J., Marques, A. C., Martins, R., Fortunato, E., & Costa, F. M. (2018). Laser-Induced Graphene Strain Sensors Produced by Ultraviolet Irradiation of Polyimide. *Advanced Functional Materials*, *28*(52). https://doi.org/10.1002/adfm.201805271

Chen, Z. P., Ren, W. C., Gao, L. B., Liu, B. L., Pei, S. F., & Cheng, H. M. (2011). Three-dimensional flexible and conductive interconnected graphene networks grown by chemical vapour deposition. *Nature Materials*, *10*(6), 424-428. https://doi.org/10.1038/Nmat3001

Cheng, C., Wang, S. T., Wu, J. N., Yu, Y. C., Li, R. Z., Eda, S., Chen, J. G., Feng, G. Y., Lawrie, B., & Hu, A. M. (2016). Bisphenol A Sensors on Polyimide Fabricated by Laser Direct Writing for Onsite River Water Monitoring at Attomolar Concentration. *ACS Applied Materials & Interfaces*, *8*(28), 17784-17792. https://doi.org/10.1021/acsami.6b03743

Cheng, Y., Wang, R., Sun, J., & Gao, L. (2015). A Stretchable and Highly Sensitive Graphene-Based Fiber for Sensing Tensile Strain, Bending, and Torsion. *Adv Mater*, *27*(45), 7365-7371. https://doi.org/10.1002/adma.201503558

Chhetry, A., Sharifuzzaman, M., Yoon, H., Sharma, S., Xuan, X., & Park, J. Y. (2019). MoS2-Decorated Laser-Induced Graphene for a Highly Sensitive, Hysteresis-free, and Reliable Piezoresistive Strain Sensor. *ACS Applied Materials & Interfaces*, *11*(25), 22531-22542. https://doi.org/10.1021/acsami.9b04915

Chyan, Y., Ye, R. Q., Li, Y. L., Singh, S. P., Arnusch, C. J., & Tour, J. M. (2018). Laser-Induced Graphene by Multiple Lasing: Toward Electronics on Cloth, Paper, and Food. *ACS Nano*, *12*(3), 2176-2183. https://doi.org/10.1021/acsnano.7b08539

Duy, L. X., Peng, Z., Li, Y., Zhang, J., Ji, Y., & Tour, J. M. (2018). Laser-induced graphene fibers. *Carbon*, *126*, 472-479. https://doi.org/10.1016/j.carbon.2017.10.036

Ferrari, A. C., & Robertson, J. (2000). Interpretation of Raman spectra of disordered and amorphous carbon. *Physical Review B*, *61*(20), 14095-14107. https://doi.org/DOI 10.1103/PhysRevB.61.14095

Fleischmann, S., Mitchell, J. B., Wang, R. C., Zhan, C., Jiang, D. E., Presser, V., & Augustyn, V. (2020). Pseudocapacitance: From Fundamental Understanding to High Power Energy Storage Materials. *Chemical Reviews*, *120*(14), 6738-6782. https://doi.org/10.1021/acs.chemrev.0c00170

Griesche, C., Hoecherl, K., & Baeumner, A. J. (2021). Substrate-Independent Laser-Induced Graphene Electrodes for Microfluidic Electroanalytical Systems. *Acs Applied Nano Materials*, *4*(3), 3114-3121. https://doi.org/10.1021/acsanm.1c00299

Jeong, S. Y., Ma, Y. W., Lee, J. U., Je, G. J., & Shin, B. S. (2019). Flexible and Highly Sensitive Strain Sensor Based on Laser-Induced Graphene Pattern Fabricated by 355 nm Pulsed Laser. *Sensors (Basel)*, *19*(22). https://doi.org/10.3390/s19224867

Kang, D., Pikhitsa, P. V., Choi, Y. W., Lee, C., Shin, S. S., Piao, L. F., Park, B., Suh, K. Y., Kim, T. I., & Choi, M. (2014). Ultrasensitive mechanical crack-based sensor inspired by the spider sensory system. *Nature*, *516*(7530), 222-226. https://doi.org/10.1038/nature14002

Lamberti, A., Clerici, F., Fontana, M., & Scaltrito, L. (2016). A Highly Stretchable Supercapacitor Using Laser-Induced Graphene Electrodes onto Elastomeric Substrate. *Advanced Energy Materials*, *6*(10). https://doi.org/ARTN 1600050
10.1002/aenm.201600050

Li, L., Zhang, J. B., Peng, Z. W., Li, Y. L., Gao, C. T., Ji, Y. S., Ye, R. Q., Kim, N. D., Zhong, Q. F., Yang, Y., Fei, H. L., Ruan, G. D., & Tour, J. M. (2016). High-Performance Pseudocapacitive Microsupercapacitors from Laser-Induced Graphene. *Advanced Materials*, *28*(5), 838-845. https://doi.org/10.1002/adma.201503333

Lin, J., Peng, Z., Liu, Y., Ruiz-Zepeda, F., Ye, R., Samuel, E. L., Yacaman, M. J., Yakobson, B. I., & Tour, J. M. (2014). Laser-induced porous graphene films from commercial polymers. *Nat Commun*, *5*, 5714. https://doi.org/10.1038/ncomms6714

Mahmood, F., Zhang, C., Xie, Y. C., Stalla, D., Lin, J., & Wan, C. X. (2019). Transforming lignin into porous graphene via direct laser writing for solid-state supercapacitors. *Rsc Advances*, *9*(39), 22713-22720. https://doi.org/10.1039/c9ra04073k

Mahmood, F., Zhang, H., Lin, J., & Wan, C. (2020). Laser-Induced Graphene Derived from Kraft Lignin for Flexible Supercapacitors. *ACS Omega*, *5*(24), 14611-14618. https://doi.org/10.1021/acsomega.0c01293

Mishra, S., Kim, Y. S., Intarasirisawat, J., Kwon, Y. T., Lee, Y., Mahmood, M., Lim, H. R., Herbert, R., Yu, K. J., Ang, C. S., & Yeo, W. H. (2020). Soft, wireless periocular wearable electronics for real-time detection of eye vergence in a virtual reality toward mobile eye therapies. *Science Advances*, *6*(11). https://doi.org/ARTN eaay1729
10.1126/sciadv.aay1729

Park, J. J., Hyun, W. J., Mun, S. C., Park, Y. T., & Park, O. O. (2015). Highly stretchable and wearable graphene strain sensors with controllable sensitivity for human motion monitoring. *ACS Appl Mater Interfaces*, *7*(11), 6317-6324. https://doi.org/10.1021/acsami.5b00695

Rahimi, R., Ochoa, M., Yu, W. Y., & Ziaie, B. (2015). Highly Stretchable and Sensitive Unidirectional Strain Sensor via Laser Carbonization. *ACS Applied Materials & Interfaces*, *7*(8), 4463-4470. https://doi.org/10.1021/am509087u

Tan, K. W., Jung, B., Werner, J. G., Rhoades, E. R., Thompson, M. O., & Wiesner, U. (2015). Transient laser heating induced hierarchical porous structures from block copolymer-directed self-assembly. *Science*, *349*(6243), 54-58. https://doi.org/10.1126/science.aab0492

Tao, L. Q., Tian, H., Liu, Y., Ju, Z. Y., Pang, Y., Chen, Y. Q., Wang, D. Y., Tian, X. G., Yan, J. C., Deng, N. Q., Yang, Y., & Ren, T. L. (2017). An intelligent artificial

throat with sound-sensing ability based on laser induced graphene. *Nature Communications*, *8*. https://doi.org/ARTN 14579
10.1038/ncomms14579
Tehrani, F., & Bavarian, B. (2016). Facile and scalable disposable sensor based on laser engraved graphene for electrochemical detection of glucose. *Scientific Reports*, *6*. https://doi.org/ARTN 27975
10.1038/srep27975
Tiliakos, A., Ceaus, C., Iordache, S. M., Vasile, E., & Stamatin, I. (2016). Morphic transitions of nanocarbons via laser pyrolysis of polyimide films. *Journal of Analytical and Applied Pyrolysis*, *121*, 275-286. https://doi.org/10.1016/j.jaap.2016.08.007
Tokonami, S., Shiigi, H., & Nagaoka, T. (2012). Molecularly Imprinted Overoxidized Polypyrrole Films for Sensor Applications from Enantiorecognition to Trace Analysis. *Molecularly Imprinted Sensors: Overview and Applications*, 73-89. https://doi.org/10.1016/B978-0-444-56331-6.00004-9
Tolvanen, J., Hannu, J., & Jantunen, H. (2018). Stretchable and Washable Strain Sensor Based on Cracking Structure for Human Motion Monitoring. *Scientific Reports*, *8*. https://doi.org/ARTN 13241
10.1038/s41598-018-31628-7
Wang, S. T., Yu, Y. C., Li, R. Z., Feng, G. Y., Wu, Z. L., Compagnini, G., Gulino, A., Feng, Z. L., & Hu, A. M. (2017). High-performance stacked in-plane supercapacitors and supercapacitor array fabricated by femtosecond laser 3D direct writing on polyimide sheets. *Electrochimica Acta*, *241*, 153-161. https://doi.org/10.1016/j.electacta.2017.04.138
Wang, Y., Yang, T. T., Lao, J. C., Zhang, R. J., Zhang, Y. Y., Zhu, M., Li, X., Zang, X. B., Wang, K. L., Yu, W. J., Jin, H., Wang, L., & Zhu, H. W. (2015). Ultra-sensitive graphene strain sensor for sound signal acquisition and recognition. *Nano Research*, *8*(5), 1627-1636. https://doi.org/10.1007/s12274-014-0652-3
Yang, T. T., Jiang, X., Zhong, Y. J., Zhao, X. L., Lin, S. Y., Li, J., Li, X. M., Xu, J. L., Li, Z. H., & Zhu, H. W. (2017). A Wearable and Highly Sensitive Graphene Strain Sensor for Precise Home-Based Pulse Wave Monitoring. *Acs Sensors*, *2*(7), 967-974. https://doi.org/10.1021/acssensors.7b00230
Ye, R., Chyan, Y., Zhang, J., Li, Y., Han, X., Kittrell, C., & Tour, J. M. (2017). Laser-Induced Graphene Formation on Wood. *Adv Mater*, *29*(37). https://doi.org/10.1002/adma.201702211
Ye, R., James, D. K., & Tour, J. M. (2019). Laser-Induced Graphene: From Discovery to Translation. *Adv Mater*, *31*(1), e1803621. https://doi.org/10.1002/adma.201803621
Zhang, J. B., Zhang, C. H., Sha, J. W., Fei, H. L., Li, Y. L., & Tour, J. M. (2017). Efficient Water-Splitting Electrodes Based on Laser-Induced Graphene. *ACS Applied Materials & Interfaces*, *9*(32), 26840-26847. https://doi.org/10.1021/acsami.7b06727
Zhang, W. L., Lei, Y. J., Ming, F. W., Jiang, Q., Costa, P. M. F. J., & Alshareef, H. N. (2018). Lignin Laser Lithography: A Direct-Write Method for Fabricating 3D Graphene Electrodes for Microsupercapacitors. *Advanced Energy Materials*, *8*(27). https://doi.org/ARTN 1801840

10.1002/aenm.201801840
Zhang, Z. C., Song, M. M., Hao, J. X., Wu, K. B., Li, C. Y., & Hu, C. G. (2018). Visible light laser-induced graphene from phenolic resin: A new approach for directly writing graphene-based electrochemical devices on various substrates. *Carbon, 127*, 287-296. https://doi.org/10.1016/j.carbon.2017.11.014